Thermodynamic and Spectroscopic Characterization of the Berenil and Pentamidine Complexes with the Dodecanucleotide d(CGCGATATCGCG)$_2$

Hans-Uwe Schmitz, Wigand Hübner and Theodor Ackermann

Abteilung Physikalische Chemie, Universität Freiburg i. Br., Albertstraße 23 a, D-79104 Freiburg i. Br., Bundesrepublik Deutschland

This paper is dedicated to the 80th anniversary of Professor Ewald Wicke

Z. Naturforsch. **50 c,** 263–274 (1995); received December 1, 1994

Berenil, Pentamidine, Differential Scanning Calorimetry, UV Absorbance Spectroscopy, FT-IR Spectroscopy

The dodecanucleotide d(CGCGATATCGCG)$_2$ was characterized by thermodynamic and UV-spectrophotometric measurements. A van't Hoff enthalpy of $\Delta H^{uv}_{v.H.} \sim -190$ kJ/mol was determined for the thermal transition using UV spectroscopy. This value was confirmed by differential scanning calorimetry (DSC). In addition we obtained the thermodynamic data $\Delta H^{DSC} = -405.1$ kJ/mol, $\Delta S^{DSC} = -1290$ J/mol·K and $\Delta G^{DSC} = -53.2$ kJ/mol for the helix to coil transition of the dodecanucleotide. The association of berenil and the oligonucleotide was accompanied with a stabilization of the host duplex (increase in T_m) and an increase in the van't Hoff enthalpy. The berenil binding parameters ($\Delta\Delta H^{DSC} = -32.6$ kJ/mol, $\Delta\Delta S^{DSC} = -72$ J/mol·K and $\Delta\Delta G^{DSC} = -11.1$ kJ/mol) revealed significant differences compared to those of the pentamidine aggregation ($\Delta\Delta H^{DSC} = -23.7$ kJ/mol, $\Delta\Delta S^{DSC} = -53$ J/mol·K and $\Delta\Delta G^{DSC} = -7.8$ kJ/mol). The transition of the pure oligonucleotide was characterized by a substantial amount of intermediate states ($\sigma^{DSC} = 0.43$) which decreased significantly upon binding of the drugs ($\sigma^{DSC} \sim 0.80$). The structural features of the complexes were analyzed by FT-IR spectroscopy. From these experiments we conclude that the configurations in the berenil and pentamidine complexes are different.

Introduction

The diarylamidines berenil (1,3-bis(4′-amidinophenyl)triazene) and pentamidine (1,5-bis(4′-amidinophenoxy)pentane) (Fig. 1) represent drugs belonging to the group of non-intercalating agents. They are known to exert mild cytotoxic, antibacterial, antihelminthic and antiviral properties [1–5] without having any significant antileucemic activity [6]. Apart from the inhibition of the polymerase reaction they are most effective against trypanosomal infections. During the last years studies involving pentamidine became of an increasing interest as it showed a significant activity against the *Pneumocystis carinii* pathogene. Pentamidine was used in the clinical treatment of *P. carinii* Pneumonia, an infection occurring in up to 80% of all Aids cases [7–11]. The detailed mechanism of the mode of action is not yet known, but there is substantial evidence for a direct interaction with the pathogene genome [12].

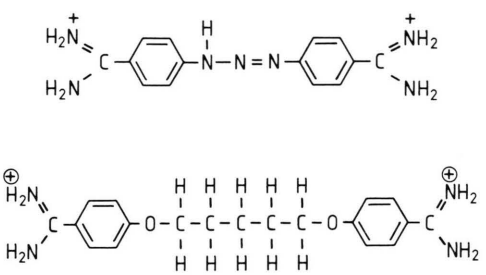

Fig. 1. Structure of berenil (1,3-bis(4′-amidinophenyl)-triazene) (top) and pentamidine (1,5-bis(4′-amidinophenoxy)pentane) (bottom).

When binding in the minor groove of double-stranded DNA a marked preference for A,T-rich sequences is observed [6] for both drug molecules. It is supposed that in addition to electrostatic interactions the complexes are stabilized by intermolecular hydrogen bonds [13–17]. The recognition of specific base sequences is possible due to the optimal fitting of the drug molecule into the minor groove. The aromatic diamidine berenil is considered to penetrate deeply with its concave side into the groove and the triazene NH group is

Reprint requests to Dr. H.-U. Schmitz.
Telefax: (0761) 203-6189.

0939–5075/95/0300–0263 $ 06.00

directed towards the bulk solvent. As a consequence hydrogen bonding of this H atom is not involved in the binding process [14, 18]. For pentamidine, in which the stiff triazene link of berenil is replaced by an aliphatic and flexible $-O(CH_2)_5O$ group a slightly altered position on the host duplex was observed [19].

In order to elucidate the correlation between the pharmacological properties of small drugs like the diarylamidines berenil or pentamidine and their specific binding to DNA a number of investigations using NMR, CD and X-ray were performed. Usually short, synthetic oligomers with 6 to 20 base pairs served as host duplexes. In this study we chose the well characterized [20] (X-ray) self-complementary dodecanucleotide $d(CGCGATATCGCG)_2$. This model system offers a four base stretch with the preferred A and T bases in the central part flanked by the two CGCG segments thus resulting in a complete turn of the helix.

Materials and Methods

Synthesis and purification of $d(CGCGATATCGCG)_2$

Berenil and pentamidine were purchased as aceturate and isethionate, respectively from Sigma and used without further purification. The concentrations were obtained spectrophotometrically using an extinction coefficient of $\varepsilon_{368} = 31{,}000 \pm 1000\ cm^{-1}\,M^{-1}$ for berenil and $\varepsilon_{260} = 28{,}500 \pm 900\ cm^{-1}\,M^{-1}$ for pentamidine. Sephadex G-10 was obtained from Pharmacia, Sweden and Fractogel TSK DEAE-650 (S) from Merck, Germany.

The oligodeoxynucleotide $d(CGCGATATCGCG)_2$ was prepared on an Applied Biosystems solid-phase DNA synthesizer (model 380 A) according to standard phosphoramidite chemistry (Institut für Biologie III, Freiburg i. Br. by G. Igloi). After detaching the DNA oligomer from the silica support the protection groups were removed by incubating in an NH_3/CH_3COOH solution (3:1, v/v) for several hours. Finally, the product was lyophilized twice from H_2O.

To separate the dodecanucleotide from small quantities of undesired side products the redissolved (H_2O) lyophilized powder was subjected to a MPLC equipped with a Fractogel DEAE-650 (S) column built in our laboratory. A linear gradient from 0 to 0.6 M KCl (2×1000 ml) in 0.01 M Tris-HCl (pH 8.5) was utilized to eluate the nucleotide. DNA was then "desalted" in a first step by application of a liquid chromatography with DEAE-650 (S) as separation medium. After washing the gel-attached nucleotide with 0.05 M TEAB (triethylamine bicarbonate) it was eluated with 1 M TEAB. The solvent was removed by rotational evaporation and redissolving twice in water. In order to obtain a completely "salt-free" compound the lyophilized probe was subsequently purified by a Sephadex G-10 column using 0.05 M TEAB. Rotational evaporation finished the last step of the preparation.

TEAB was prepared by passing CO_2 gas through a freshly distilled triethylamine solution (2 M) at 0 °C until the pH was 7.

Buffer system and nucleotide solution

All measurements were performed in a buffer system consisting of 2 mM sodium phosphate, 60 mM NaCl, 0.1 mM EDTA, adjusted to pH 7.0.

The concentration of the self-complementary oligonucleotide was determined spectrophotometrically. Extinction coefficients at 25 °C were calculated by nearest-neighbor approximation [21]. For $d(CGCGATATCGCG)_2$ we obtained a value of $\varepsilon_{260} = 9392\ cm^{-1}\,M^{-1}$. The required absorbances (DNA in the random coil conformation) of the nucleotide solutions were estimated by extrapolating the upper base line of a thermally induced transition curve (strands exist completely in the single-stranded state) to 25 °C. All concentrations mentioned throughout the text are given in moles of double-strands.

UV/VIS absorbance spectroscopy

Spectroscopic measurements were performed with a Perkin-Elmer Lambda 7 UV/VIS Spectrophotometer using cuvettes with path lengths of 0.100–1.000 cm. In all experiments the registered absorbances were in the range of 0.5 to 1.8. The temperature was controlled by means of a home-built digital device connected with a Peltier element integrated in the cuvette holder. The UV "melting" profiles were recorded at 260 nm with an x-y recorder and subsequently digitized as ASCII files. The heating rate was 1 °C/min. Below

12 °C the cuvette chamber was purged with nitrogen to avoid condensation. In order to extract thermodynamic data from the optical transition curves a series of experiments over a range of concentrations was conducted.

In all experiments with the "drug-free" nucleotide solutions the standard buffer was used as the reference. Measurements of nucleotide solutions containing berenil or pentamidine were corrected by subtracting the reference spectrum of the drug solution with an equal concentration. At 260 nm changes in the drug spectrum due to the binding process were negligible compared to the absolute absorbance values of the nucleotide. Thus, the temperature induced dissociation of the ligand did not significantly disturb the UV transition curves. This could be proved by equivalent hyperchromicity values of the free and complexed oligonucleotide accompanying the "melting" of the base pairs [22].

Differential scanning calorimetry (DSC)

For DSC experiments a DASM-4 microcalorimeter [23] (V/O Mashpriborintorg, Russia) directly connected with a small computer (Atari, model 1040 STF) was used. Data collection (~1600 points per run) was possible with a serial input-output system developed in our laboratory. The temperature was scanned from 5 °C to 90 °C at a rate of 1 °C/min. For each experiment at least two independent measurements were recorded. Furthermore, temperature scans were repeated twice for the same probe. The calorimeter was equipped with a sample and a reference cell of equal volume (0.47325 ml). The reference cell was filled with buffer solution.

FT-IR spectroscopy

Experiments were performed with a Bruker IFS 113 Fourier transform infrared spectrometer equipped with a nitrogen-cooled MCT detector. A 4/86 IBM Computer served as a work station and for data processing (OS/2, opus, Bruker). Spectra with a resolution of 2 cm^{-1} were obtained by Fourier transforming a total of 1024 apodized interferograms. Subsequently, the raw spectra were smoothed and base-line corrected.

For preparation of the samples the buffered solutions were lyophilized, redissolved in deuterium oxide and lyophilized again three times to complete H/D exchange. After dissolving the samples in the initial volume of D_2O a CaF_2 cell with a path length of 100.7 μm was filled immediately. The cuvette was thermostated by an external water bath.

Results

Analysis of UV-spectroscopic data

As a prerequisite for the characterization of the drug/oligonucleotide complex a complete investigation of the thermodynamic and spectroscopic properties of the unligated duplex was indispensible. To evaluate thermodynamic data as the van't Hoff values $\Delta H^{uv}_{v.H.}$, $\Delta S^{uv}_{v.H.}$, $\Delta G^{uv}_{v.H.}$ and the "melting" temperatures the thermally induced UV transition curves (digitized as ASCII files) were normalized by subtracting of lower and upper base lines [24]. The normalized curves were transformed to θ *versus* T plots. From the plots the van't Hoff transition enthalpy $\Delta H^{uv}_{v.H.}$ is obtained by Eqn. (1) [24].

$$\Delta H^{uv,shape}_{v.H.} = (2 + 2m) \cdot RT^2_m \left(\frac{\partial\theta}{\partial T}\right)_{\theta = 0.5} . \qquad (1)$$

R denotes the gas constant and m the molecularity. θ represents the fraction of helical state and T_m is the "melting" temperature which is by definition the temperature where θ = 0.5. Fig. 2 shows the θ *versus* T plot after normalizing and transforming a transition curve of d(CGCGATATCGCG)$_2$.

The θ *vs.* T plots can be subjected to a simulation routine to obtain a calculated model curve representing the thermally induced helix to coil

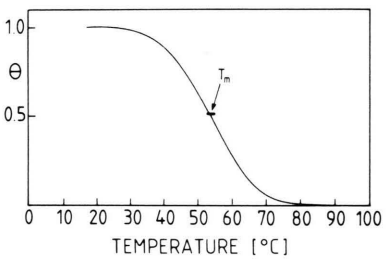

Fig. 2. θ *versus* T plot derived by normalizing a thermal UV transition curve of d(CGCGATATCGCG)$_2$ in 60 mM NaCl, 2 mM phosphate, 0.1 mM EDTA at pH 7.0. The duplex concentration was 7.6×10^{-5} M. T_m at θ = 0.5 is indicated.

transition. The degree of helix formation is given by Eqn. (2)

$$\theta = 1 + \left[4\,C_T \cdot \exp\left(-\frac{\Delta H_{v.H.}}{RT} + \frac{\Delta S_{v.H.}}{R}\right)\right]^{-1} - \sqrt{\left[4\,C_T \cdot \exp\left(-\frac{\Delta H_{v.H.}}{RT} + \frac{\Delta S_{v.H.}}{R}\right)\right]^{-2}} \quad (2)$$

which can be derived on the basis of a two-state process. In this expression C_T represents the total concentration of single-strands. The fitting procedure is accomplished by means of the Marquardt-Levenberg algorithm [25]. From optimal fittings the thermodynamic data $\Delta H_{v.H.}^{uv,sim}$ and $\Delta S_{v.H.}^{uv,sim}$ can be deduced. The change in the Gibbs energy $\Delta G_{v.H.}^{uv,sim}$ can be calculated according to the Gibbs-Helmholtz relation

$$\Delta G = \Delta H - T\Delta S. \quad (3)$$

In Fig. 3a the fit of the calculated model curve and the $\theta_{(T)}$ plot of d(CGCGATATCGCG)$_2$ is shown. In Fig. 3b the quality of the fitting routine can be checked by an illustration of the differences in $\theta_{(T)}$. The thermodynamic data resulting from this simulation were $\Delta H_{v.H.}^{uv,sim}$ = −178.8 kJ/mol and $\Delta S_{v.H.}^{uv,sim}$ = −470 J/mol·K. Using expression 3 we calculated $\Delta G_{v.H.}^{uv,sim}$ = −38.8 kJ/mol at 25 °C.

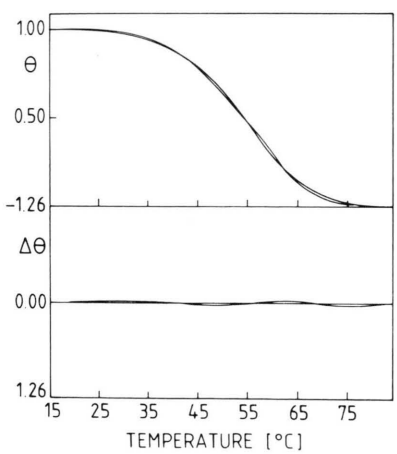

Fig. 3. Top: Simulation of the θ *versus T* plot constructed from the thermal denaturation curve (UV) of d(CGCGATATCGCG)$_2$. The fitting procedure is based on a two-state model (Eqn. (2), see text) and the experimental conditions were as outlined in Fig. 2. Bottom: The quality of the simulation routine can be checked by the temperature-dependent difference of the θ values between the experimental curve and the fit.

Alternatively the van't Hoff transition enthalpy is accessible by application of Eqn. (4):

$$\Delta H_{v.H.}^{uv,tdiff} = \frac{B}{\left(\frac{1}{T_{max}} - \frac{1}{T_{3/4}}\right)}. \quad (4)$$

Here, B represents a value which is a function of the reaction molecularity (see Table I), T_{max} is the temperature at the maximum of the differentiated transition curve [26, 27]. $T_{3/4}$ is the three quarter transition temperature ($(\partial\theta/\partial T)$ = 0.5 $(\partial\theta/\partial T)_{max}$). For comparison the van't Hoff transition enthalpies derived by Eqns (1) and (4) ($\Delta H_{v.H.}^{uv,shape}$ = −189 kJ/mol and $\Delta H_{v.H.}^{uv,tdiff}$ = −192 kJ/mol) are listed in Table II. Obviously, these data are in good agreement with the values deduced from the simulation routine.

Apart from the fitting procedure which is based on Eqn. (2) the $\Delta S_{v.H.}^{uv}$ values can be obtained in a different way. A second method [28] sometimes leading to deviating results, is based on concentration-dependent experiments. For self-complemen-

Table I. Calculated B-values (J/mol·K) as a function of the molecularity m (used in Eqn. (4)).

Molecularity m	Constant B
1	−14.65
2	−18.33
3	−21.19

Table II. Van't Hoff transition enthalpies $\Delta H_{v.H.}^{uv,shape}$ and $\Delta H_{v.H.}^{uv,tdiff}$ as derived from UV experiments (by using Eqns (1) and (4)). The corresponding transition temperatures T_m are also indicated. The values in brackets are evaluated from measurements with decreasing temperature gradient. Duplex concentration was ~1×10^{-6} M.

Sample	$\Delta H_{v.H.}^{uv,shape}$ [kJ/mol]	T_m [°C]	$\Delta H_{v.H.}^{uv,tdiff}$ [kJ/mol]	T_m [°C]
d(CGCGATATCGCG)$_2$	−189 [−178]	54.0 [56.6]	−192 [−211]	58.9 [63.4]
Dodecamer–berenil (1:1)	−366	65.9	−397	70.9
Dodecamer–berenil (1:10)	−470	70.2	−446	72.9
Dodecamer–pentamidine (1:1)	−336	61.6	−306	65.0
Dodecamer–pentamidine (1:10)	−359	64.2	−328	66.8

tary single-strands $\Delta S^{uv}_{v.H.}$ can be calculated according to Eqn. (5):

$$\frac{1}{T_m} = \frac{(m-1)R}{\Delta H^{uv,conc}_{v.H.}} \ln C_T + \frac{[\Delta S^{uv,conc}_{v.H.} - (m-1)R \cdot \ln 2 + R \cdot \ln(m)]}{\Delta H^{uv,conc}_{v.H.}} \quad (5)$$

A plot of $1/T_m$ *versus* $\ln C_T$ should give a straight line which allows moreover calculating the van't Hoff transition enthalpy. In Fig. 4 a diagram for d(CGCGATATCGCG)$_2$ is shown. From a line calculated by a least-square fit we determined a value of $\Delta H^{uv,conc}_{v.H.} = -306.3$ kJ/mol of cooperative unit, $\Delta S^{uv,conc}_{v.H.} = -846$ J/mol·K and using Eqn. (3) $\Delta G^{uv,conc}_{v.H.} = -54.1$ kJ/mol at $T = 25$ °C. Unfortunately, there is a substantial discrepancy between the data obtained by application of Eqn. (5) and the analysis of the shape of the transition curves (Eqns (1) and (4)). The main reason causing this fact is attributed to the inherent base-line problem introduced by the normalization of the experimental UV curve. This feature clearly demonstrates the basic influence of the applied procedure on the absolute values. Hence, a comparison of results determined by different methods should be treated carefully as was already pointed out in the literature [24].

The addition of berenil or pentamidine to a solution of d(CGCGATATCGCG)$_2$ altered the thermodynamic data significantly. The drug/duplex ratios adjusted in the experiments were 1:1 and 10:1. The balanced ratio (1:1) is used to create a complex with the ligated molecule bound in the minor groove of the central part of the helix (ATAT). This configuration with a binding site of 3 to 5 base pairs [29] was proved by means of

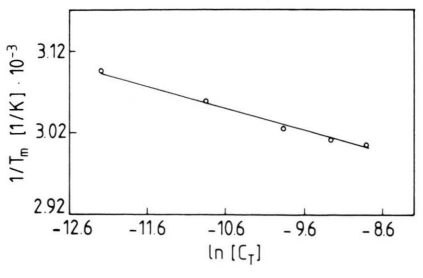

Fig. 4. $1/T_m$ *versus* $\ln C_T$ plot for d(CGCGATATCGCG)$_2$ in 60 mM NaCl, 2 mM phosphate, 0.1 mM EDTA, pH 7.0.

NMR [15, 16] and X-ray [13, 14] studies of berenil/pentamidine oligonucleotide complexes. The GC flanking regions are known to offer less attractive binding sites mainly attributed to the sterical hindrance in the minor groove by the exocyclic amino group of the guanine bases. From comparative studies of complexes between berenil and the polynucleotides poly-d(AT) or poly-d(G-C) [30] this selectivity could be quantified by the binding constants differing in at least one order of magnitude.

In Table II the van't Hoff transition enthalpies and "melting" temperatures determined according to Eqns (1) and (4) are listed for the complexes. Data extracted from transition curves of the free nucleotide obtained by decreasing the temperature with a rate of 1 °C/min from 80 °C to 10 °C are given in brackets. Within experimental error these values were identical to those obtained from the heating curves.

The addition of berenil to the nucleotide solution (1:1) is followed by an increase in the transition temperature of ~11 °C (Table II) while the van't Hoff enthalpy changes from ~ −190 kJ/mol to ~ −380 kJ/mol. A 10-fold excess of berenil over the duplex concentration results in intensified effects with respect to the pure dodecanucleotide. The transition temperature of the complex is ~71 °C and thus approximately 4 °C higher compared to the value established for the 1:1 complex. The $\Delta H^{uv}_{v.H.}$ value of ~ −460 kJ/mol cooperative unit determined for berenil–d(CGCGATATCGCG)$_2$ (10:1 input ratio) differs drastically from ~ −380 kJ/mol in the adduct with a balanced drug/nucleotide input ratio. These significant effects indicate incomplete saturation in the presence of a low drug concentration and higher "binding densities" (bound ligands per duplex) with an excess of ligand. Complete saturation is achieved at a 10:1 input ratio, which was deduced from nearly constant T_m values and van't Hoff enthalpies observed for drug/duplex ratios higher than 10:1. Varying berenil concentrations below this ratio were followed by significant changes. The association constant of ~10^6 M^{-1} obtained for the related berenil–poly-d(AT) complex [22] indicates the strong affinity of berenil to the helical ATAT segment. Therefore, already at low berenil concentrations the binding site in the central part of the minor groove is covered to a

high degree. The additional stabilization (→ ΔT_m values) can only be explained by the interaction of ligand molecules with the vacant but less attractive binding sites in the minor groove of the CGCG flanks.

The results derived from analogue experiments with the diarylamidine pentamidine are also listed in Table II. The binding process is accompanied by qualitatively equivalent changes, *e.g.* higher "melting" temperatures and increased van't Hoff enthalpies but the observed trends are less pronounced. The increase of the T_m values demonstrating the duplex stabilization induced by the ligand pentamidine is less than 8 °C in the 1:1 adduct and smaller than 10 °C in the complex with an excess of ligand. For the van't Hoff transition enthalpies values of ~ −320 kJ/mol (1:1 input ratio) and ~ −345 kJ/mol (10:1 input ratio) are obtained exhibiting a moderate effect upon binding compared to the interaction of berenil.

Analysis of the calorimetric data

Thermodynamic binding profile

The helix to coil transition of the dodecanucleotide d(CGCGATATCGCG)$_2$ is characterized by the thermodynamic data ΔH^{DSC}, ΔS^{DSC} and ΔG^{DSC}. They can be evaluated directly from the calorimetric transition curves. These data are determined model-independent and the same analysis is applicable in the presence of berenil or pentamidine. In Fig. 5 the base-line corrected DSC heating curve of the berenil–d(CGCGATATCGCG)$_2$ aggregate is shown.

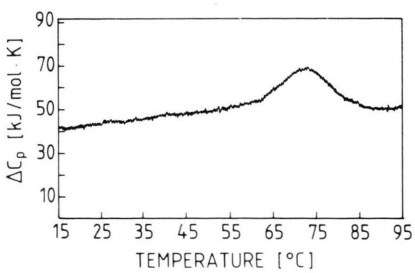

Fig. 5. Temperature-induced helix to coil transition curve (DSC) of the berenil–d(CGCGATATCGCG)$_2$ complex (1:1). The nucleotide concentration was 5.3×10^{-5} M in 60 mM NaCl, 2 mM phosphate, 0.1 mM EDTA at pH 7.0. The curve indicates the change in molar heat capacity *versus* temperature after base-line correction.

The area under the heat absorption peak is proportional to the enthalpy change ΔH^{DSC} induced by the thermal transition of the nucleotide [28]:

$$\Delta H^{DSC} = \int_{T_A}^{T_E} \Delta C_p dT. \quad (6)$$

The associated entropy change ΔS^{DSC} can be derived by integration following Eqn. (7):

$$\Delta S^{DSC} = \int_{T_A}^{T_E} \frac{\Delta C_p}{T} dT. \quad (7)$$

Application of the general thermodynamic relationship given in Eqn. (3) allows the calculation of the change in the Gibbs energy ΔG^{DSC}. The integration was accomplished using a straight line between the integration limits. These were determined by UV spectroscopy experiments performed under identical conditions [31]. Data evaluated comparatively considering smoothed curves and non-linear base-lines (spline functions) for the integration were in good agreement. Prior to integration all experimental transition curves were base-line corrected.

A quantitative estimate of the binding parameters was obtained in a straightforward analysis by subtracting the values describing the thermal transition of the free duplex from those derived for the ligated deoxynucleotide. The resulting $\Delta\Delta H^{DSC}$, $\Delta\Delta S^{DSC}$ and $\Delta\Delta G^{DSC}$ values are listed in Table III as well as the corresponding thermodynamic data ΔH^{DSC}, ΔS^{DSC} and ΔG^{DSC}.

The complete thermodynamic profile of the free dodecanucleotide is ΔH^{DSC} = −405.1 kJ/mol duplex, ΔS^{DSC} = −1290 J/mol·K and ΔG^{DSC} = −53.2 kJ/mol. Our experimentally determined enthalpy value can be compared with a theoretical estimate calculated using enthalpy increments for the base pairs. Following the models of Delcourt and Blake [32], Doktycz and Benight [33] and Breslauer [34] we obtained −417 kJ/mol, −412 kJ/mol and −440 kJ/mol, respectively, which are in acceptable agreement with our experimental data. Adding the diarylamidine berenil to the nucleotide substantially influences the thermodynamic properties. This is clearly evidenced by the $\Delta\Delta H^{DSC}$, $\Delta\Delta S^{DSC}$ and $\Delta\Delta G^{DSC}$ values (Table III). The stabilization of the helix is accompanied with a negative enthalpy change of −32.6 kJ/mol in the 1:1 complex and −74.4 kJ/mol in the saturated complex (10:1 input ratio). With

Table III. Thermodynamic data ΔH^{DSC}, ΔS^{DSC} and ΔG^{DSC} derived from the DSC experiments. The binding parameter $\Delta\Delta H^{DSC}$, $\Delta\Delta S^{DSC}$ and $\Delta\Delta G^{DSC}$ for the complexes are given in the last three columns. The changes in the Gibbs energy are calculated for 25 °C and the drug/duplex input ratios are indicated. The buffer contained 2 mM phosphate, 0.1 mM EDTA, 60 mM NaCl at pH 7.0 and the duplex concentration was $\sim 1\times10^{-4}$ M.

Sample	ΔH^{DSC} [kJ/mol]	ΔS^{DSC} [J/mol·K]	ΔG^{DSC} [kJ/mol]	$\Delta\Delta H^{DSC}$ [kJ/mol]	$\Delta\Delta S^{DSC}$ [J/mol·K]	$\Delta\Delta G^{DSC}$ [kJ/mol]
Dodecamer	−405.1	−1218	−42.1	–	–	–
Dodecamer–berenil (1:1)	−437.7	−1290	−53.2	−32.6	−72	−11.1
Dodecamer–berenil (1:10)	−479.5	−1377	−68.9	−74.4	−159	−26.8
Dodecamer–pentamidine (1:1)	−428.8	−1271	−49.9	−23.7	−53	−7.8

−23.7 kJ/mol this effect is less significant for the pentamidine aggregate. In all investigated complexes the entropy changes upon ligand binding are negative. This is mainly attributed to the reduction of the overall number of molecules in the solution due to the complexation.

The $\Delta\Delta G^{DSC}$ values calculated for 25 °C confirm the results derived from the optical measurements (UV). Berenil exhibits a stronger stabilization of the helix than the analogue pentamidine (−11.1 kJ/mol *versus* −7.8 kJ/mol). An increase of the ligand/base pair ratio is followed by an additional stabilization effect due to the higher degree of saturation. This was also concluded from the inspection of the transition temperatures.

Characterization of the transition

The calorimetric transition curves can readily be transformed to $\theta_{(T)}$ plots which allow the analysis of van't Hoff enthalpies according to the Eqns (1) or (4). Considering that the van't Hoff enthalpies are derived assuming a two-state model, whereas the calorimetrically determined ΔH^{DSC} values are model-independent, the ratio $\sigma^{DSC} = \Delta H^{DSC}_{v.H.}/\Delta H^{DSC}$ provides a measure of the size of the cooperative unit (see Table IV). It may also be taken as a criterion whether the helix to coil transition occurs in a two-state ($\sigma^{DSC} = 1$) or multi-state ($\sigma^{DSC} < 1$) process. Intermolecular reactions result in σ^{DSC} values higher than 1. In Table IV the data obtained from our DSC experiments are listed. For the free dodecanucleotide a σ^{DSC} value of 0.43 suggests a high degree of populated intermediates. The all-or-none model is definitely not applicable for this thermally induced transition. This result basically might explain the relatively high discrepancy in the van't Hoff enthalpies evaluated spectroscopically (Eqn. (5)) and calorimetrically. The addition of berenil or pentamidine increases the cooperativity of the transition ($\Delta H^{DSC}_{v.H.}$ increases) and the σ^{DSC} values indicate less intermediates ($\sigma^{DSC} = 0.78$; $\sigma^{DSC} = 0.83$). Thus, the transition approaches an all-or-none process in the presence of a ligand.

Table IV. Van't Hoff transition enthalpies and T_m values derived from the DSC measurements. In the last column the calculated size of the cooperative unit σ^{DSC} is indicated (for experimental conditions see Table III).

Sample	$\Delta H^{DSC}_{v.H.}$ [kJ/mol]	T_m [°C]	σ^{DSC}
Dodecamer	−175.1	61.3	0.43
Dodecamer–berenil (1:1)	−338.2	69.8	0.78
Dodecamer–pentamidine (1:1)	−357.3	66.2	0.83
Dodecamer–berenil (1:10)	−419.0	76.1	0.87

Analysis of FT-IR absorbance spectra

The absorbance spectra of nucleotides in D_2O solution exhibit several bands in the range of 1750 cm^{-1} to 1550 cm^{-1}. These bands are mainly attributed to the ring breathing modes of the purine and pyrimidine rings (~1575 cm^{-1} for GC base pairs; ~1625 cm^{-1} for AT base pairs), to the carbonyl stretching mode at the C_4 position of thymine residues (~1660 cm^{-1}) and to the D_2=O stretching mode of the pyrimidine bases thymine and cytosine [35, 36] (~1690 cm^{-1}). The wavenumber of the band maxima $\tilde{\nu}_{max}$ and the integral band intensities I_{max} depend on the hydrogen bonding behavior of the base pairs and thus directly reflect the characteristics of the helix conformation. Additional hydrogen bonds occurring upon the complexation reaction with drug molecules should influence the band pattern in the spectra as well [37]. For this reason FT-IR spectroscopy provides a

helpful tool in the investigation of structural features of biomolecules.

The bandwidth of individual absorption components was substantially larger than their separation in wavenumbers thus leading to overlapping effects in the IR spectra. In order to evaluate the desired data the smoothed and base-line corrected spectra were subjected to a Fourier self-deconvolution procedure [38–40]. Using a lorentzian lineshape with a band half-width of $\omega = 20\ cm^{-1}$ and a resolution enhancement factor of $k = 1.8$ as input parameters we obtained an adequate separation of the overlapping bands. Subsequently, the "band-narrowed" spectra were underlayed with a minimum number of gaussian bands which were coadded to give a synthetic spectrum. The synthetic component bands were then adjusted by gradually varying two adjustable parameters (ω and position of band maximum $\tilde{\nu}_{max}$) to minimize the difference between the calculated and original deconvoluted spectrum. An optimal refinement was accomplished in the last step by an automated least-square routine.

Fig. 6 shows the deconvoluted D_2O spectra of d(CGCGATATCGCG)$_2$, the corresponding berenil complex (1:1) and the pentamidine complex (1:1) registered at 15 °C (solid lines). The component bands representing the best refinement of the fitting procedure are underlayed (dashed lines).

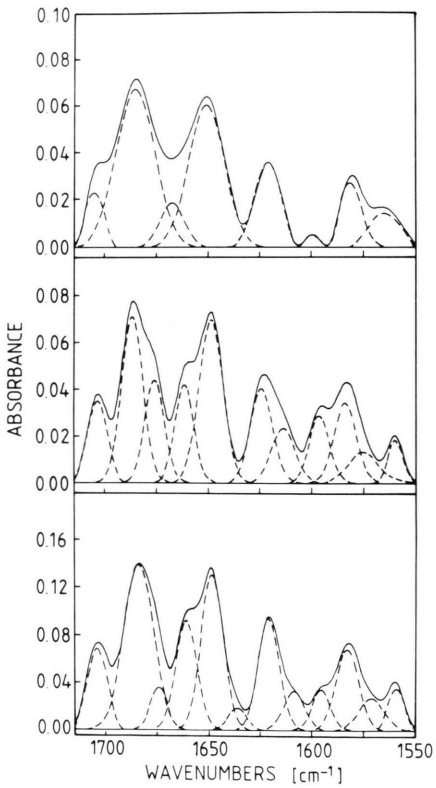

Fig. 6. Top: Fourier-self-deconvoluted infra-red D_2O spectrum of d(CGCGATATCGCG)$_2$ (solid line) and individual component bands (dashed lines) obtained by the curve fitting procedure (see text). In the middle the deconvoluted berenil–dodecamer (1:1) D_2O spectrum is shown with component bands. The deconvoluted spectrum of the pentamidine–d(CGCGATATCGCG)$_2$ complex (1:1) with component bands is illustrated at the bottom. The deconvolution was performed with a lorentzian lineshape using the parameters $\omega = 20\ cm^{-1}$ and $k = 1.8$; the spectra were recorded at 15 °C in 60 mM NaCl, 2 mM phosphate, 0.1 mM EDTA.

Table V. Results of the curve fitting procedure for the D_2O spectrum of the dodecanucleotide in 2 mM phosphate, 0.1 mM EDTA, 60 mM NaCl at 15 °C. Listed are the band positions $\tilde{\nu}_{max}$, the half-widths ω, the integral and the relative band intensities (I_{max}, I).

d(CGCGATATCGCG)$_2$			
$\tilde{\nu}_{max}$ [cm^{-1}]	ω [cm^{-1}]	I_{max}	I [%]
1704.5	11.8	0.42	6.88
1685.1	21.9	1.85	30.58
1667.2	13.6	0.31	5.21
1650.6	20.4	1.53	25.3
1620.5	15.6	0.71	11.67
1599.1	9.7	0.11	1.79
1581.1	12.5	0.42	6.96
1564.5	20.6	0.47	7.82
1536.8	9.8	0.08	1.40
1527.1	11.0	0.15	2.40

Table VI. Results of the curve fitting procedure for the D_2O spectra of the complexes (1:1) in 2 mM phosphate, 0.1 mM EDTA, 60 mM NaCl at 15 °C. Listed are the band positions $\tilde{\nu}_{max}$, the half-widths ω, the integral and the relative band intensities (I_{max}, I).

Berenil complex				Pentamidine complex			
$\tilde{\nu}_{max}$ [cm^{-1}]	ω [cm^{-1}]	I_{max}	I [%]	$\tilde{\nu}_{max}$ [cm^{-1}]	ω [cm^{-1}]	I_{max}	I [%]
1703.1	11.5	0.48	8.22	1703.9	12.9	1.11	9.82
1686.7	12.2	0.98	16.89	1683.7	16.8	2.62	23.30
1675.8	11.2	0.56	9.60	1674.2	8.9	0.36	3.18
1661.5	10.6	0.50	8.68	1660.9	11.9	1.23	10.88
1648.6	13.6	1.07	18.35	1648.4	12.5	1.85	16.36
–	–	–	–	1636.2	10.5	0.22	1.91
1624.1	12.7	0.58	9.99	1621.9	12.1	1.27	11.26
1613.5	13.2	0.35	6.01	1608.7	12.2	0.44	3.92
1596.3	11.4	0.37	6.37	1595.3	10.3	0.39	3.45
1583.8	12.8	0.49	8.48	1582.9	12.7	0.98	8.67
1575.3	16.1	0.25	4.24	1571.4	14.5	0.42	3.75
1559.8	8.7	0.19	3.18	1559.5	9.2	0.39	3.49

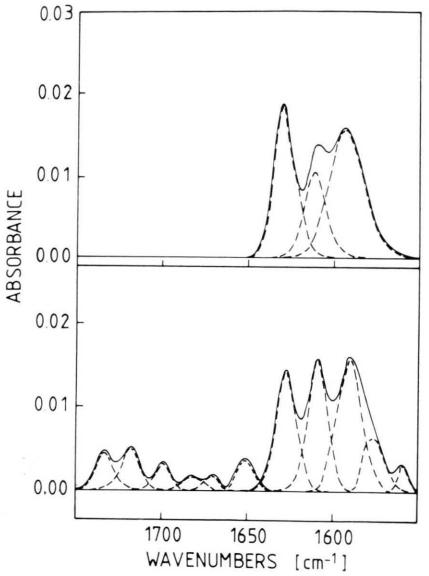

Fig. 7. Deconvoluted D_2O spectra of berenil (solid line, top) and pentamidine (solid line, bottom) with underlayed component bands (dashed lines) derived by the curve fitting analysis (see text).

The extracted data for the dodecanucleotide and the complex spectra are listed in Tables V and VI, respectively. For the sake of comparison the relative band intensities I (%) are given in the last columns. The deconvoluted spectra of berenil and pentamidine (Fig. 7) reveal stronger absorptions only in the wavenumber range from 1640 cm^{-1} to 1550 cm^{-1}. A detailed interpretation of this selected part of the spectra is omitted because the overlapping of various bands (nucleotides, drug molecules) obscurred an exact and specific assignment. However, between 1750 cm^{-1} and 1640 cm^{-1} there are no significant contributions of the ligand and the complex spectra can be analyzed straightforward [41].

By inspection of the spectra we noticed that the complexation is obviously followed by changes in the range of 1750 cm^{-1} to 1640 cm^{-1}. The most striking effect upon binding is the splitting of the band at 1667 cm^{-1} into two bands located at ~1661 cm^{-1} and ~1675 cm^{-1}. The spectrum of the free oligonucleotide doesn't exhibit any bands at these positions. The integral intensities of the two appearing bands are remarkably different in the berenil and pentamidine adduct spectra. This can be illustrated comparing the intensity ratio of I_{1675}/I_{1661} with values of 1.1 for the berenil complex and 0.3 for the pentamidine complex.

An important aspect concerning the location of interaction on a molecular level is obtained by examination of the band situated at 1685.1 cm^{-1}. In the spectrum of the berenil complex this band shifts upwards to 1686.7 cm^{-1} (Tables V and VI). The spectrum of the pentamidine complex reveals an absorbance maximum $\tilde{\nu}_{max}$ at 1683.7 cm^{-1} and in both cases the half-widths ω decreases. Since this band is assigned to the C_2=O stretching mode of the thymine bases which is not involved in the Watson-Crick base pairing, this particular spectral change indicates an intermolecular ligand/base interaction rather than a conformational distortion of the oligonucleotide.

Discussion

It was already mentioned that it might be hazardous to compare absolute van't Hoff values evaluated by different procedures. Especially the data analysis of UV-spectroscopic experiments depends seriously on the applied techniques [42]. This fact becomes rather obvious in the comparison of the van't Hoff transition enthalpies. Nevertheless, an interpretation of the data derived by the same method is feasible if only relative changes are regarded. Following this, our UV experiments clearly indicate an increase of van't Hoff transition enthalpies upon binding. Obviously, the bound ligand molecule induces a more cooperative "melting" of the base pairs. In the first phase of the temperature increase the dissociation rate of base pairs is low because of the stabilization effect; after the break up of the complex (duplex-ligand) a cooperative dissociation of base pairs immediately takes place. This effect is more evident in the berenil–d(CGCGATATCGCG)$_2$ adduct ($\Delta H^{uv}_{v.H.}$ ~ −380 kJ/mol) than in the pentamidine complex ($\Delta H^{uv}_{v.H.}$ ~ −320 kJ/mol). Combined with the observation that the duplex stabilization is more pronounced for berenil than for pentamidine (T_m values, Table II) we conclude that the binding of berenil to the model oligomer is favoured. This difference is attributed to the enlarged molecular length of 19 Å for pentamidine [2]. It doesn't fit perfectly into the binding site of four AT base pairs because the GC flanks with their exocyclic amino groups (guanine) pointing

into the minor groove sterically disfavour the pentamidine interaction [19, 43]. In contrast, berenil with a molecular length [6] of 14 Å is able to penetrate deeply into the minor groove [44]. A higher saturation of the dodecanucleotide (10:1 drug/base pair ratio) results in an additional increase of this differences between the complexes and the pure oligomer as seen by the changes in T_m values and numerically higher van't Hoff enthalpies (Table II).

From the calorimetric investigations we extract a more quantitative interpretation of the comparative binding study. The association of berenil to the duplex (1:1) is followed by an enthalpy change of $\Delta\Delta H^{DSC} = -32.6$ kJ/mol. This is in an acceptable agreement with the reported value of −28.8 kJ/mol derived from binding studies [22] with the alternating polymer poly-d(AT) and the theoretically calculated value of −36.8 kJ/mol [45]. With a negative binding entropy of $\Delta\Delta S^{DSC} = -71$ J/mol·K an overall stabilization of $\Delta\Delta G^{DSC} = -11.1$ kJ/mol is obtained. Compared to $\Delta\Delta G^{DSC} = -7.8$ kJ/mol (pentamidine adduct) the change in the Gibbs energy confirms thermodynamically the stronger stabilizing effects of berenil. Although the calorimetric data for the pentamidine complex exhibit a less negative entropy term ($\Delta\Delta S^{DSC} = -53$ J/mol·K) the smaller concomitant binding enthalpy of $\Delta\Delta H^{DSC} = -23.7$ kJ/mol allows only a relatively low complex stability. Since the entropic contribution is negative in all investigated cases, the binding enthalpy ΔH^{DSC} can definitely be regarded as the driving force for the complexation. Marky *et al.* [46] discussed a value of $\Delta H^{DSC} = -8$ kJ/mol to $\Delta H^{DSC} = -13$ kJ/mol per hydrogen bond, so that at least two H bonds seem to be involved in the interaction.

The increase of the drug concentration to a 10-fold over the duplex concentration affects the binding parameters and enforces a saturation of the binding sites with ligands. The helix is stabilized by $\Delta\Delta H^{DSC} = -74.4$ kJ/mol, for $\Delta\Delta S^{DSC}$ we determined −159 J/mol·K and $\Delta\Delta G^{DSC}$ can be calculated to −26.8 kJ/mol at 25 °C (Table III). Assuming that under these experimental conditions two additional berenil molecules are bound to the GC flanks (saturation) and neglecting any ligand–ligand interaction, each of these two molecules stabilizes the helix with a $\Delta\Delta G^{DSC}$ value of approximately −20 kJ/mol. This result matches perfectly with the binding enthalpy of −21 kJ/mol derived for the homopolymeric berenil–poly-(dG)·poly-(dC) complex [47].

DSC experiments can also be used to determine the van't Hoff transition enthalpies. The value obtained for the free nucleotide $\Delta H^{DSC}_{v.H.} = -175.1$ kJ/mol (Eqn. (1), Table IV) is in good agreement with the UV-spectroscopically derived value of −189 kJ/mol (Table II). Adding berenil or pentamidine to the nucleotide solution yields van't Hoff enthalpies numerically larger than −330 kJ/mol which confirms the optical results. This directly reflects the cooperative "melting" process of the base pairs as outlined in the previous section. σ^{DSC} values allow an additional characterization of the transition in the absence and presence of ligand. Table IV shows that the pure double-stranded nucleotide dissociates by populating a substantial amount of intermediate states ($\sigma^{DSC} = 0.43$). Upon binding of the drug molecule the σ^{DSC} value approaches ~0.80 indicating a trend towards an all-or-none behavior. Summarizing the calorimetric data, we conclude that the addition of berenil or pentamidine stabilizes the helical conformation of the duplex, increases the cooperativity of the "melting" process and the length of the cooperative unit, whereas the amount of intermediate states decreases. Hence, the thermal transition of the drug–dodecanucleotide complex exhibits more characteristics of a two-state process than the dissociation of the pure nucleotide duplex.

The thermodynamic and UV-spectroscopic results indicate significant changes upon the binding of the small ligands berenil and pentamidine. A more detailed understanding of the structural features of the dodecanucleotide-ligand aggregate on a molecular basis is obtained by FT-IR spectroscopy. The splitting of the band at 1667 cm^{-1} (Tables V and VI) into two well separated bands reflects substantial changes in the Watson-Crick hydrogen bonding system (C_4=O stretching mode of thymine). Unfortunately, it is not possible to clarify whether this effect is the consequence of conformational distortions of the core helix and/or if it must be attributed to ligand-helix interactions. From X-ray studies [13, 14, 16, 19] using very similar base sequences of the oligomers it is known that the penetration of small ligands into the minor groove is accompanied by conformational distortions of the helices. In this adducts the struc-

ture of the host duplexes shows propeller twisting, tilt of the bases and different values for the helix parameters as winding angle or width of grooves. Thus, our IR result underlines the probability of potential distortions of the helix conformation in oligonucleotide/drug complexes.

The calculated ratios of the integral band intensities I_{1675}/I_{1661} (1.1 and 0.3) exhibit additional information. They implicate a different structural situation in the berenil and the pentamidine complex. Despite the high topological similarities of the two drug molecules the binding behavior is not identical. This observation makes it plausible that the two related derivates exhibit quite different pharmacological activities.

The band located at 1685.1 cm^{-1} in the free oligonucleotide is shifted to 1686.7 cm^{-1} in the berenil complex and to 1683.7 cm^{-1} (Tables V and VI) in the pentamidine aggregate. As already mentioned above this band is attributed to the C_2=O stretching mode of the pyrimidine residues which is not involved in Watson-Crick base pairing. The wavenumber variation of this band in the complexes reflects ligand-base interactions. This result reconciles with observations of closely related complexes using NMR or X-ray. From the different direction of the band shifts in our IR spectra we again conclude that the binding configuration is not exactly the same in the berenil and the pentamidine aggregates.

Concluding Remarks

Our results clearly show that the diarylamidines berenil and pentamidine, only differing in the bridging central part of the molecules exhibit a comparable behavior upon binding to oligonucleotides. Both drugs bind in the minor groove and stabilize the helical conformation of the host duplex. Nevertheless, we found significant differences in the thermodynamic and the structural properties of the complexes. In order to develop efficient antibiotics a detailed knowledge of the thermodynamic aspects for complexation reactions and of the specific molecular features introducing the varying pharmacological potential is indispensable.

[1] H. W. Zimmermann, Angew. Chem. **98,** 115 (1986); Angew. Chem., Int. Ed. Engl. **25,** 115 (1986).
[2] L. L. Bennett Jr., Prog. Exp. Tumor Res. **7,** 259 (1965).
[3] J. Anné, E. De Clercq, H. Eyssen, and O. Dann, Antimicrob. Agents Chemother. **18,** 231 (1980).
[4] I. Snapper, J. Amer. Med. Ass. **133,** 157 (1947).
[5] E. De Clercq and O. Dann, J. Med. Chem. **23,** 787 (1980).
[6] B. C. Baguley, Mol. Cell. Biochem. **43,** 167 (1982).
[7] A. B. Montgomery, J. M. Luce, J. Turner, E. T. Lin, R. J. Debs, K. J. Corkery, E. N. Brunette, and P. C. Hopewell, Lancet ii **1987,** 480.
[8] B. G. Gazzard, J. Antimicrob. Chemother. **23,** 67 (1989).
[9] J. A. Golden, D. Chernoff, H. Hollander, D. Feigal, and J. E. Conte, Lancet i **1989,** 654.
[10] B. Wispelwey and R. D. Pearson, Infect. Control. Hosp. Epidemiol. **12,** 375 (1991).
[11] M. Sands, M. A. Kron, and R. B. Brown, Ref. Infect. Dis. **7,** 625 (1985).
[12] R. R. Tidwell, S. K. Jones, J. D. Geratz, K. H. Ohemeng, M. Corey, and J. E. Hall, J. Med. Chem. **33,** 1252 (1990).
[13] D. G. Brown, M. R. Sanderson, E. Garman, and S. Neidle, J. Mol. Biol. **226,** 481 (1992).
[14] D. G. Brown, M. R. Sanderson, J. V. Skelly, T. C. Jenkins, T. Brown, E. Garman, D. I. Stuart, and S. Neidle, EMBO J. **9,** 1329 (1990).
[15] S. Hu, K. Weisz, T. L. James, and R. H. Shafer, Eur. J. Biochem. **204,** 31 (1992).
[16] A. N. Lane, T. C. Jenkins, T. Brown, and S. Neidle, Biochemistry **30,** 1372 (1991).
[17] L. H. Pearl, J. V. Skelly, and B. D. Hudson, Nucl. Acids Res. **15,** 3469 (1987).
[18] N. Gresh and B. Pullman, Molec. Pharmacol. **25,** 452 (1984).
[19] K. J. Edwards, T. C. Jenkins, and A. Neidle, Biochemistry **31,** 7104 (1992).
[20] M. A. F. F. de C. T. Carrondo, M. Coll, J. Aymani, A. H.-J. Wang, G. A. Marel, J. H. van Boom, and A. Rich, Biochemistry **28,** 7849 (1989).
[21] P. N. Borer, Handbook of Biochemistry and Molecular Biology (G. D. Fasman, ed.), 3rd Edition, p. 589, CRP Press, Cleveland, U.S.A. 1975.
[22] H.-U. Schmitz and W. Hübner, Biophys. Chem. **48,** 61 (1993).
[23] P. L. Privalov, Pure Appl. Chem. **52,** 479 (1980).
[24] K. J. Breslauer, Thermodynamic Data for Biochemistry and Biotechnology (H. J. Hinz, ed.), p. 402, Springer Verlag, Berlin, Heidelberg, New York, Tokyo 1986.

[25] W. H. Press, B. P. Flannery, S. A. Teukolsky, and W. T. Vetetling, Numerical Recipes – The art of scientific computing, Cambridge University Press, Cambridge 1986.
[26] J. Gralla and D. M. Crothers, J. Mol. Biol. **73,** 497 (1973).
[27] L. A. Marky, L. Canuel, R. A. Jones, and K. J. Breslauer, Biophys. Chem. **13,** 141 (1981).
[28] L. A. Marky and K. J. Breslauer, Biopolymers **26,** 1601 (1987).
[29] M. J. Waring, Mol. Subcell. Biol. **2,** 216 (1969).
[30] Ch. Zimmer and U. Wähnert, Prog. Biophys. Molec. Biol. **47,** 31 (1986).
[31] J. Ohms and Th. Ackermann, Biophys. Chem. **34,** 137 (1989).
[32] S. G. Delcourt and R. D. Blake, J. Mol. Biol. **28,** 15160 (1991).
[33] M. J. Doktycz, R. F. Goldstein, T. M. Paner, F. J. Gallo, and A. S. Benight, Biopolymers **32,** 849 (1992).
[34] K. J. Breslauer, R. Frank, H. Blöcker, and L. A. Marky, Proc. Natl. Acad. Sci. **83,** 3746 (1986).
[35] H. T. Miles and J. Frazier, Biochem. Biophys. Res. Commun. **14,** 21 (1964).
[36] H. T. Miles and J. Frazier, J. Mol. Biol. **162,** 219 (1982).
[37] E. Taillandier, J. Liquier, and M. Ghomi, J. Mol. Struct. **214,** 185 (1989).
[38] J. K. Kauppinen, D. J. Moffatt, H. H. Mantsch, and D. G. Cameron, Appl. Spectrosc. **35,** 271 (1981).
[39] J. K. Kauppinen, D. J. Moffatt, H. H. Mantsch, and D. G. Cameron, Appl. Opt. **20,** 1866 (1981).
[40] J. K. Kauppinen, D. J. Moffatt, H. H. Mantsch, and D. G. Cameron, Anal. Chem. **53,** 1454 (1981).
[41] H.-U. Schmitz and W. Hübner, Fifth International Conference on the Spectroscopy of Biological Molecules (Th. Theophanides, J. Anastassopoulou, and N. Fotopoulos, eds.) (1993).
[42] C. E. Longfellow, R. Kierzek, and D. H. Turner, Biochemistry **29,** 278 (1990).
[43] K. R. Fox, C. E. Sansom, and M. F. G. Stevens, FEBS Lett. **266,** 155 (1990).
[44] F. Gago, Ch. A. Reynolds, and W. G. Richards, Molec. Pharmacol. **35,** 232 (1988).
[45] K. Zakrzewska, R. Lavery, and B. Pullman, Nucl. Acids Res. **12,** 6559 (1984).
[46] L. A. Marky, J. G. Snyder, and K. J. Breslauer, Nucl. Acids Res. **11,** 5701 (1983).
[47] H.-U. Schmitz, Dissertation, University of Freiburg, Germany (1994).